Improving Mitral Repair for Functional Mitral Regurgitation

A Thesis
Presented to
The Academic Faculty

by

Grason K. Gasser

In Partial Fulfillment
of the Requirements for the Degree

B.S. in Biomedical Engineering with Research Option
in the School of Biomedical Engineering

Georgia Institute of Technology
January 2020

Improving Mitral Repair for Functional Mitral Regurgitation

Approved by:

Paul Fincannon, Research Option Undergraduate Coordinator
School of Biomedical Engineering
Georgia Institute of Technology

Muralidhar Padala

Digitally signed by Muralidhar Padala
DN: cn=Muralidhar Padala, o=Emory University, ou=Cardiothoracic Surgery, email=spadala@emory.edu, c=US
Date: 2020.04.25 16:20:42 -05'00'

Dr. Muralidhar Padala
Program Faculty in Biomedical Engineering
Georgia Institute of Technology

Dr. Wei Sun
Associate Professor in Biomedical Engineering
Georgia Institute of Technology

Date Approved:

ACKNOWLEDGEMENTS

I would like to first thank my parents, Kelly and Jason Gasser for their constant support through not only my college career, but life as well. This project would not have been possible without the guidance I received from Dr. Padala and training from Dongyang Xu.

TABLE OF CONTENTS

LIST OF TABLES

LIST OF FIGURES

LIST OF SYMBOLS AND ABBREVIATIONS

MR	Mitral regurgitation
IMR	Ischemic mitral regurgitation
LV	Left ventricle
CAD	Coronary artery disease
CHF	Congestive heart failure
LVEF	Left ventricular ejection fraction
LVEDD	Left ventricular end-diastolic diameter
PL	Posterior leaflet
UMA	Undersized Mitral Annuloplasty
PMA	Papillary Muscle Approximation
IPMS	Inter-Papillary Muscle Separation
LVSV	Left Ventricular Stroke Volume

ABSTRACT

Ischemic mitral regurgitation is affiliated with changes in annular dimensions as well as remodeling of the left ventricle. Undersized mitral annuloplasty (UMA), which involves implanting a titanium-based ring-like structure onto the mitral annulus, is aimed at reducing annular dimensions in order to restore leaflet coaptation and therefor correct IMR. The durability of this treatment is improved with papillary muscle approximation (PMA), in which a suture draws together the two papillary muscles that connect the mitral valve to the heart muscle, reducing the lateral separation of the papillary muscles in order to relieve tethering on the mitral leaflets to correct IMR. The participants in this investigation are retrospectively identified patients who have already undergone surgery for IMR. The purpose of this retrospective study is to investigate (1) the impact UMA has on left ventricular function and (2) whether preoperative geometry, specifically inter-papillary muscle separation (IPMS), is predictive of FMR severity at 12 months after UMA.

CHAPTER 1

INTRODUCTION

Mitral Regurgitation

The human heart has four valves, two on the left side and two on the right side, which help maintain unidirectional blood flow and efficient cardiac pumping. The mitral valve, located on the left side between the left atrium and left ventricle (LV), can become prone to leaking. This disease state, known as mitral regurgitation (MR), is a structural heart pathology described as the backflow of blood into the left atrium due to insufficient closing of the valve leaflets during systole. This condition can subsequently lead to dysfunction of the left ventricle, which could ultimately result in heart failure[1]. The pathology can be either primary MR due to an organic dysfunction of a portion of the valve itself, or secondary MR which originates from LV remodeling[2]. More specifically, ischemic mitral regurgitation (IMR) arises from complications with left ventricular remodeling due to coronary artery disease or following myocardial infarction (MI), as is the case in approximately one-fifth of patients[2,3]. IMR is associated with decreased long-term survival rates in patients post MI and is present in 10% of patients with coronary artery disease (CAD). Overall, 70% of congestive heart failure (CHF) cases in the U.S are due to cardiomyopathy (diseases of the heart muscle) and 50% of those cases involve patients with IMR. This totals to a range of 1.6 to 2.8 million cases of IMR in the United States alone[4-7]. The pathology of this disease state will now be discussed in greater detail.

IMR can be distinguished by tethering of the posterior leaflet, primary history of MI, restricted leaflet motion in systole, and annular dilation associated with LV remodeling.

In the diseased state, the mitral valve will also lose its saddle-like shape and become flattened. Displacement of the papillary muscles increases the tethering force on the leaflets, while decreased ventricular function leads to decreased closing forces, as seen in Figure 1. These factors interfere with systolic closing, which can lead to regurgitation. The impairment of lateral shortening between papillary muscles determines the severity of MR[8,9].

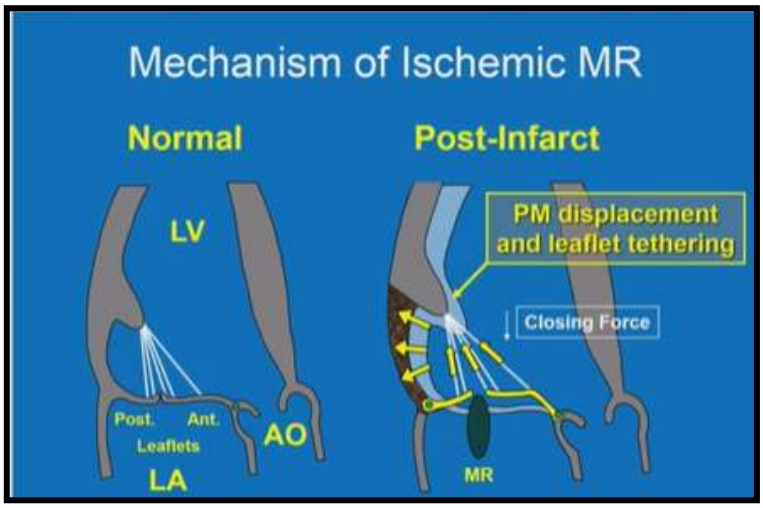

Figure 1: Demonstration of the effects of papillary muscle impairment and tethering as indicators of IMR after MI. Regurgitation results from disruption of the opening and closing forces[4].

Undersized Mitral Valve Annuloplasty and Papillary Muscle Approximation

As annular dilation is almost always present in patients with IMR, undersized mitral valve annuloplasty (UMA), a simple and reproducible procedure, is currently considered the gold standard of treatment. This surgical approach aims to restore native annulus geometry, prevent further dilation, and increase coaptation surface of the leaflets[10,11]. The ring used in this procedure is normally at least two sizes smaller than that of the original

valve in order to obtain a coaptation length of at least 8 mm[10]. A full-size ring (instead of a partial ring) is more common in IMR patients to help reduce the possibility of recurrence[12,13]. This procedure was first used in a study conducted by Bach et al. on a cohort of 9 patients. The report alludes to observing recovery of left ventricular function, as transformation of LV shape is a substrate for development of IMR[14].The overall symptoms of all patients showed marked improvement (effective correction of mitral regurgitation confirmed by color flow Doppler imaging), but more research was needed in order to generalize the results to a broader population.[15,16] Some of the more recent literature has also highlighted adverse effects of restrictive annuloplasty, such as a possible creation of functional mitral stenosis associated with higher pulmonary arterial pressure and worse functional capacity.[17-19]

Because excessive annular reduction by UMA can lead to mitral stenosis and worse functional capacity, papillary muscle approximation (PMA) has been recently suggested to be coupled with UMA. PMA relieves leaflet tethering by drawing together the two muscles that connect the mitral valve to the heart muscle, reducing inter-papillary muscle separation so aggressively that UMA may not be necessary for IMR correction[20-23]. This reduction in interpapillary muscle distance (IPMD) helps to restore leaflet coaptation[24,25]. The major findings of a study conducted by Nappi et al. revealed higher rates of MR reappearance in patients who had undergone UMA alone compare to those who had undergone PMA (55.9% recurrence vs. 27% respectively in a 5-year follow up period).[26] Overall, the study aims to determine the best surgical technique for treatment of IMR, as there is currently not a single technique established as more successful than the other.

If the patient is appropriately selected, UMA alone, or a combination of UMA + PMA, promotes reverse remodeling of the LV[26] and improves overall quality of life. The best candidates for this procedure are in the early phases of the disease with a short history of heart failure, do not have an excessively dilated left ventricle, and have no echocardiographic evidence of potential recurrence of MR[4,27,28]. This study investigated the use of these techniques in patients with IMR in order to examine the first hypothesis that correction utilizing UMA improves left ventricular function.

Preoperative Selection of Patients

Surgeons must preoperatively evaluate patients in order to determine the likelihood of a positive outcome with undersized annuloplasty. There are factors that increase a patient's chances of being selected for this kind of surgical repair because of the inclination towards positive postoperative outcomes. For example, patients with less severe tethering and increased left ventricular ejection fraction (LVEF) are favored because they have more treatable MR and can tolerate increased cross clamp time[4]. Also, in patients with preoperative left ventricular end-diastolic diameter (LVEDD) that exceeds 65 mm, the five-year survival rate is significantly lower than patients with LVEDD of 65 mm or less (49% vs. 80% respectively)[12]. Additional analysis of the preoperative mitral valve configuration has indicated that in patients undergoing restrictive annuloplasty, the posterior leaflet (PL) angle (as can be seen in Figure 2) may be the strongest predictor of postoperative outcomes[29]. A PL angle of ≥45 degrees has been associated with lower 3-year event free survival (22±17% vs. 76±12%)[30].

Figure 2: Evaluation of the posterior leaflet angle as a preoperative parameter for indicating outcomes for undersized annuloplasty to correct IMR. Other factors evaluated via echocardiography included anterior leaflet angle, coaptation distance, and tenting area.[29]

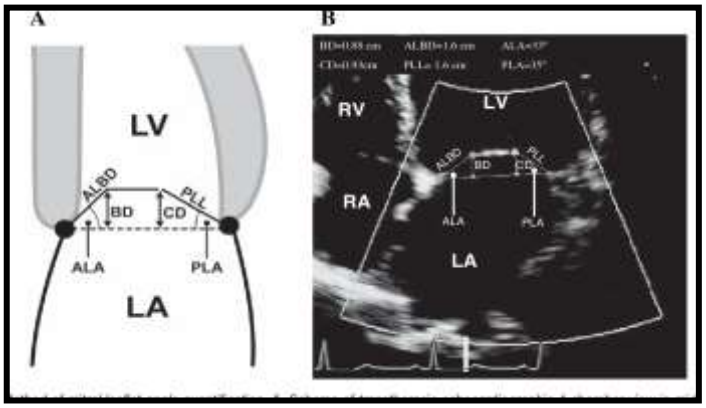

Echocardiography, Magnetic Resonance Imaging (MRI) and Strain Analysis

Echocardiography is the main method used to visually evaluate cardiac function, as well as diagnose chronic IMR[7,31]. Ultrasound waves create images of the heart, which can be translated into different views for assessing mitral valve and ventricular pathologies. The essential views for assessment of the mitral valve will now be discussed. The *parasternal long axis* view shows thickness of the leaflets and their motion during cardiac cycling. With this view, mitral valve tenting area (the area between the annular line and the leaflets), coaptation distance (distance between annular line and coaptation point), and posterior leaflet angle (inverse sine of CD/PLL per Figure 2) can be measured[29]. Visualization of the left atrium is also available.

Mitral leaflet motion and their attachment to the chordae is visible in the *parasternal short axis* view. Mitral valve area can also be measured from this image. Coaptation of both mitral valve leaflets as well as LV diastolic parameters can be assessed via *the apical four chamber* view (as seen in Figure 3). This is of particular use for evaluating left ventricular function following restrictive annuloplasty. The degree of possible mitral regurgitation and evaluation of different segments of the leaflets is best done with the *apical long axis* or "three chamber" view[32]. Quantitatively, MR may also be assessed

using the width of the vena contracta (narrowest portion of color jet) of the regurgitant jet and ratio of MR color jet area to LA area[29].

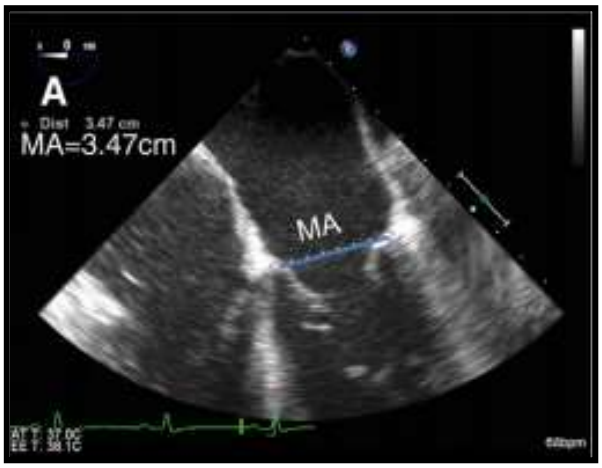

Figure 3: Mitral valve in four chamber view in order to measure the annulus[32].

MRI holds the standard for noninvasive measurement of ventricular size and function[33]. The accuracy of this method for calculating ventricular volumes is based on the ability to choose the imaging plane, eliminating the need for assumptions of geometry. Quantification of left and right ventricular stroke volume is done by segmenting the ventricles from the base to the apex of the heart in end-diastole and end-systole as seen in Figure 4 (basal, equatorial, and apical slices). This has important clinical applications, as reliable detection of changes in cardiac chamber size can be used as a guide for surgical intervention and timing of MV therapies[34]. MR can also be measured based on quantitative flow, as mitral regurgitant volume is calculated as the difference between left ventricular stroke volume (LVSV) and forward flow[33]. LV remodeling and reverse remodeling after intervention can also be visualized with MRI.

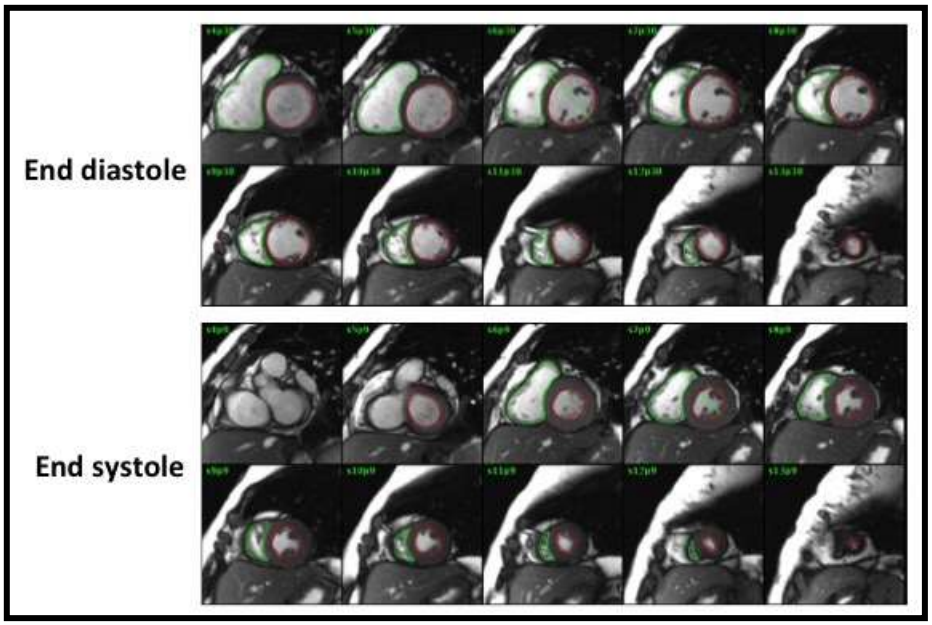

Figure 4: Segmentation of the ventricles from base to the apex in both end-diastole and end-systole[35].

LV function can be quantified through the principle of myocardial strain, which describes local changes in myocardial thickness (as observed through MRI in this investigation)[36,37]. In the case of short axis views, strains from each LV segment can only be calculated along circumferential and radial directions. Left ventricular ejection fraction (LVEF) is the most consistent physiological predictor of adverse outcomes for regurgitant valvular disease cases[1]. In short, reduced LVEF indicates decreased myocardial contractility, a late consequence of the disease which can imply irreversible damage to the myocardium[1]. The current shift in clinical settings is to use strain imaging to identify this injury at an early stage, before reduction in ejection fraction. However, there is a need for more randomized trials which investigate strain imaging as a closer predictor of depressed LV function. This study utilizes strain analysis to investigate the hypothesis that preoperative LV geometry determines leaflet mobility.

CHAPTER 2

METHODS AND MATERIALS

Ethical Considerations

Patient data was collected through the Society of Thoracic Surgeons database at Emory Hospital. A certificate through the Collaborative Institutional Training Initiative was obtained for "Biomedical Research Investigators and Key Personnel" by this investigator and submitted to the International Review Board before access to patient data was granted.

Study Design

This is a retrospective subset of an interventional clinical trial with total estimated enrollment of 140 participants aged 18 years or older. The intervention-based portion of this study began March 20, 2018 and is projected to be completed by December 31, 2023. Patients were divided into three arms: UMA (Group 1), UMA+PMA (Group 2), and No Intervention (retrospectively identified patients who already underwent surgery at Emory Hospital). Retrospectively identified patients were suitable for the recruitment to this study for their post-operative investigation and were the core focus for the work done by this researcher.

The inclusion criteria for this study are as follows: patient has been diagnosed with FMR, left ventricular end diastolic diameter is less than or equal to 70mm, systolic tenting height is less than or equal to 12mm, mitral regurgitation is of moderate or greater severity (as defined by guidelines of American society of echocardiography at time of study approval), cardiomyopathy is present with ischemic or non-ischemic origins, and

patient is able to sign informed consent and release medical information forms. The exclusion criteria are as follows: any evidence of structural (chordal or leaflet) mitral lesions, planned concomitant intra-operative procedures, planned concomitant intra-operative Maze procedure for symptomatic paroxysmal atrial fibrillation, persistent atrial fibrillation, prior mitral valve repair, contraindication for cardiopulmonary bypass, clinical signs of cardiogenic shock at time or randomization, ST segment elevation myocardial infarction within 14 days prior to inclusion in this study, congenital heart disease (except PFO or ASD), chronic renal insufficiency, recent history of psychiatric disease likely to impair compliance with study protocol, and pregnancy at time of randomization.

Surgical Technique

Participants who underwent UMA received a commercially available annuloplasty ring. In this procedure, 10-12 Ethicon sutures are placed around the mitral annulus and the metallic ring is then implanted on the annulus to reduce its size. An Edwards Lifesciences Physio II ring was used in all patients with ring size ranging from 26mm to 30mm. Patients who underwent the additional treatment of PMA received one or two 4-0 pledgeted sutures used to draw the two papillary muscle tips together, reducing IPMS prior to UMA.

Outcome Measures

The primary outcome measure of this study is the change in FMR severity, evaluated using cardiac echocardiography and/or MRI. Secondary outcome measures are organized in the table below.

Table 1: Secondary outcomes and corresponding time frames.

Secondary Outcome	*Time Frame*
Mortality Rate	Post-Intervention (Up to 20 Days), Post-Intervention (Month 6), Post Intervention (Month 12)
Number of Major Adverse Cardiac Events	Duration of Study (6 Years)
Change in Quality of Life Scale Score	Baseline, Post-Intervention, Post-Intervention (Month 12)
Change in Minnesota Living with Heart Failure Questionnaire Score	Baseline, Post-Intervention (Month 6), Post-Intervention (Month 12)
Change in Functional Status Assessed by 6-Minute Walk Test	Time Frame: Baseline, Post-intervention (Month 6), Post-Intervention (Month 12)
All Cause Readmission Rate	Post-Surgery (Up to 30 Days)
Heart Failure Readmission Rate	Post-Surgery (Up to 30 Days)
Change in Left Ventricular Volume	Baseline, Post-Intervention (Month 6), Post-Intervention (Month 12)

Change in Left Ventricular Volume	Baseline, Post-Intervention (Month 12)
Change in Left Ventricular Mass	Baseline, Post-Intervention (Month 6), Post-Intervention (Month 12)
Change in Left Ventricular Mass	Baseline, Post-Intervention (Month 12)

CHAPTER 3

RESULTS

Segmentation

MRIs from all patients were anonymized before evaluation in order to prevent bias. Segment Medviso software was then used to perform segmentation of the left ventricle from end-diastolic to end-systolic phases as is demonstrated by Figure 5. Trends in myocardial thickness were determined for basal, equatorial, and apical sections. All images were taken from CINE short axis (SA) view.

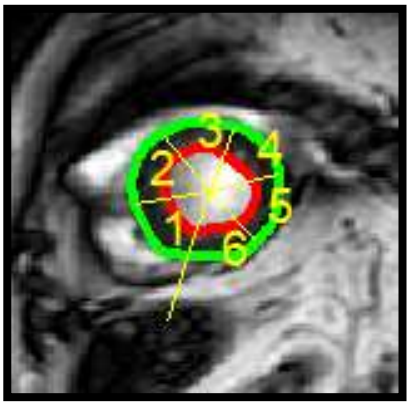

Figure 5: Apical slice demonstrating LV segmentation with 6 sectors, sector 1 being on the septal side.

Using the end-diastolic point as the initial time frame for all slices, ventricular wall thickness, fractional wall thickening, and radial velocity were determined for all patients.

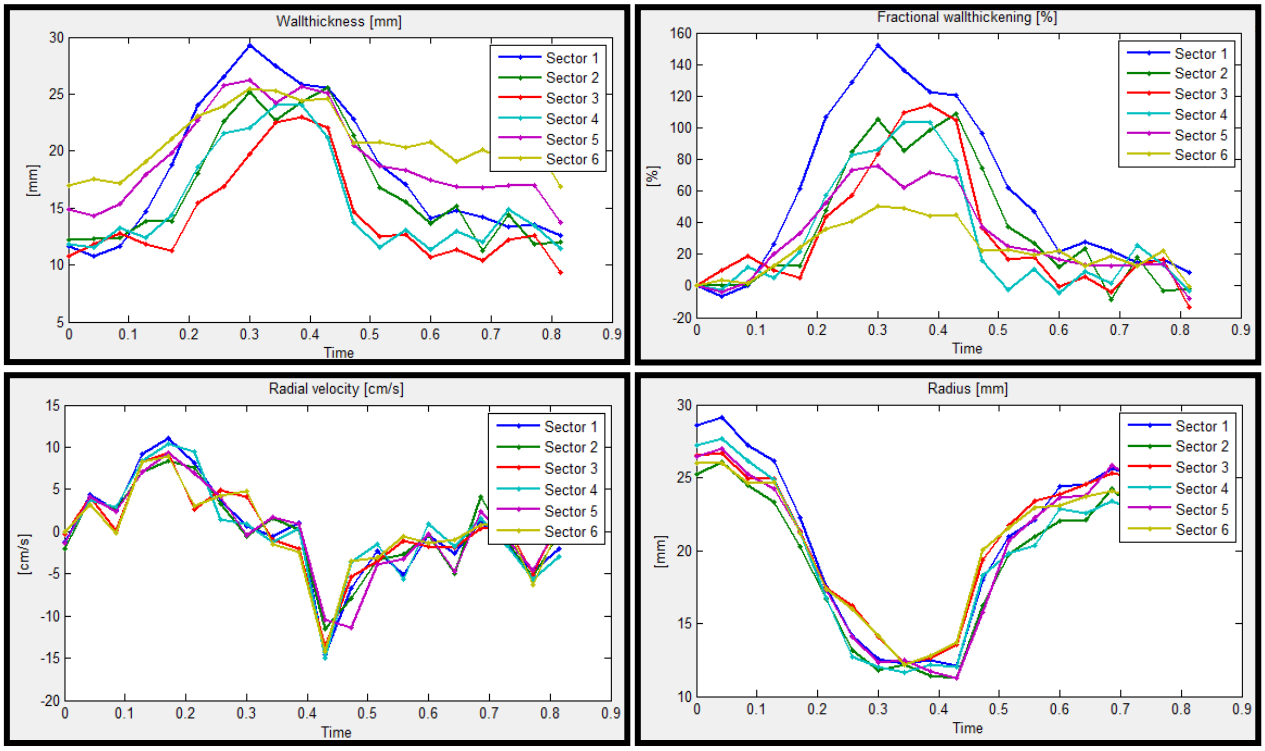

Figures 6 (top left), Figure 7 (top right), Figure 8 (bottom left), and Figure 9 (bottom right): Sample of data collected from a single representative basal slice in order to demonstrate the typical curves for wall thickness, fractional wall thickening, radial velocity, and radius.

Strain Analysis

Myocardial strain analysis, conducted using the same Segment Medviso software, was used to measure the fractional change of myocardial dimension in specific directions. This is an established method used to assess myocardial function. In Figures 10-21, mean circumferential strain and mean radial strain are plotted for basal, equatorial, and apical regions. The peak mean radial strains and and peak mean circumferential strains for all patients was then compared and collected in Table 2. For reference, the beginning time point is at the end of diastole.

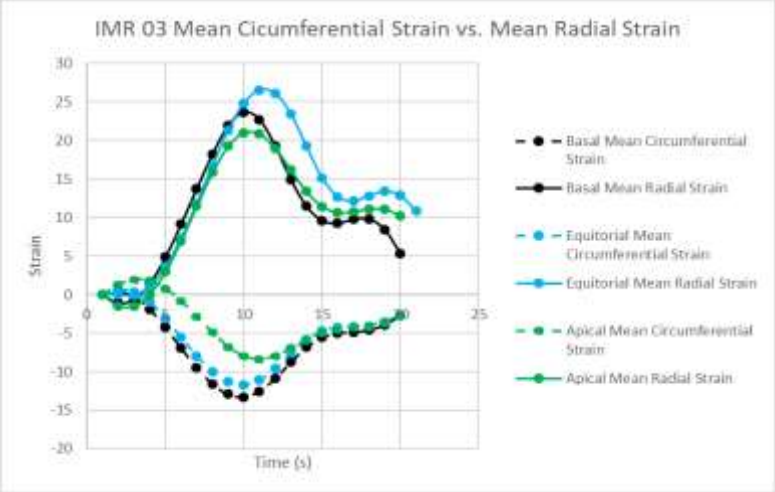
IMR 03 Mean Cicumferential Strain vs. Mean Radial Strain
Strain
Time (s)
Basal Mean Circumferential Strain
Basal Mean Radial Strain
Equitorial Mean Circumferential Strain
Equitorial Mean Radial Strain
Apical Mean Circumferential Strain
Apical Mean Radial Strain

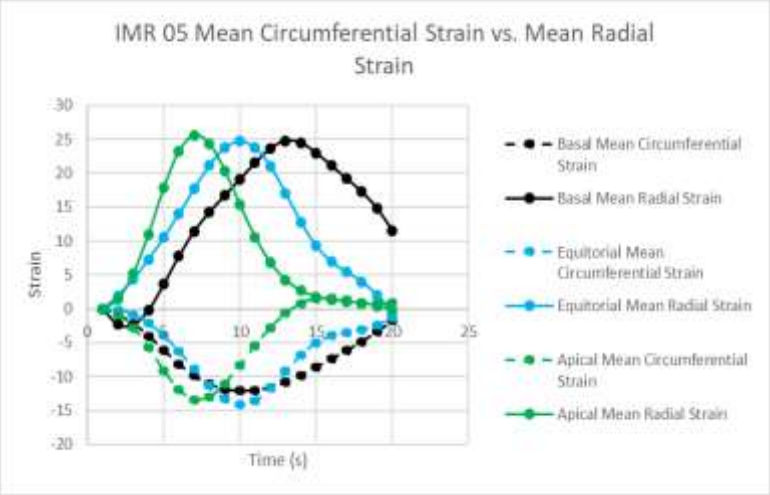
IMR 05 Mean Circumferential Strain vs. Mean Radial Strain
Strain
Time (s)
Basal Mean Circumferential Strain
Basal Mean Radial Strain
Equitorial Mean Circumferential Strain
Equitorial Mean Radial Strain
Apical Mean Circumferential Strain
Apical Mean Radial Strain

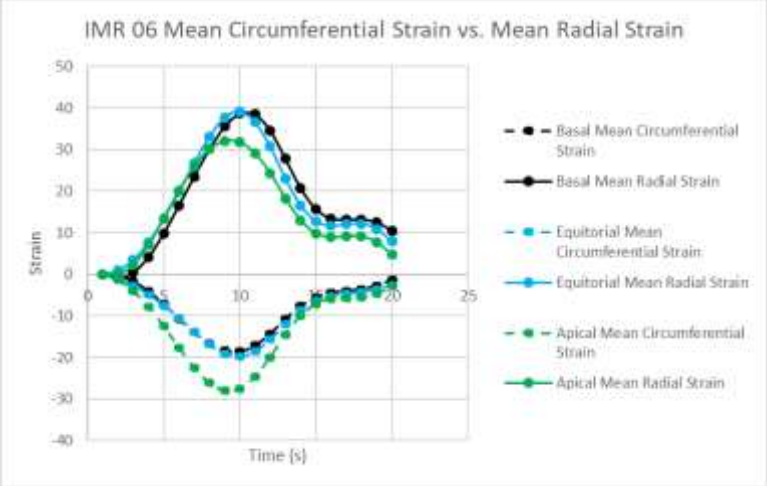
IMR 06 Mean Circumferential Strain vs. Mean Radial Strain
Strain
Time (s)
Basal Mean Circumferential Strain
Basal Mean Radial Strain
Equitorial Mean Circumferential Strain
Equitorial Mean Radial Strain
Apical Mean Circumferential Strain
Apical Mean Radial Strain

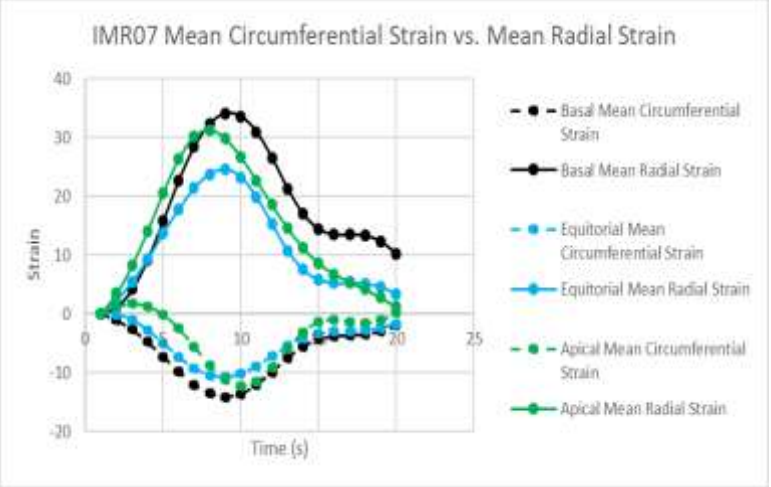
IMR07 Mean Circumferential Strain vs. Mean Radial Strain
Strain
Time (s)
Basal Mean Circumferential Strain
Basal Mean Radial Strain
Equitorial Mean Circumferential Strain
Equitorial Mean Radial Strain
Apical Mean Circumferential Strain
Apical Mean Radial Strain

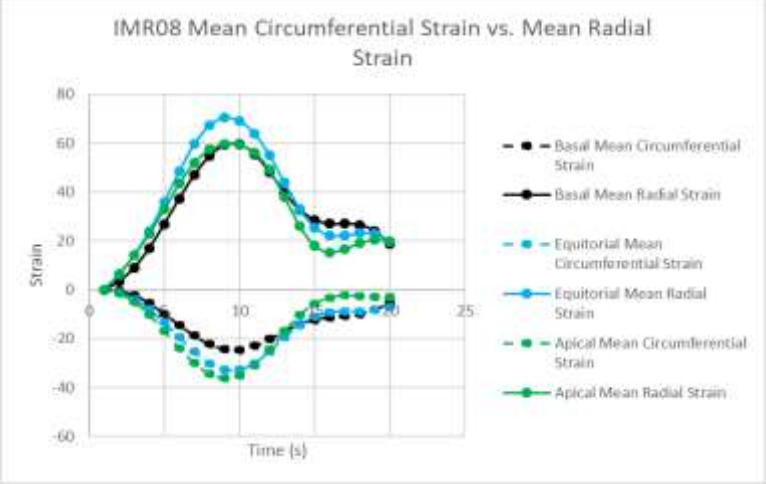
IMR08 Mean Circumferential Strain vs. Mean Radial Strain
Strain
Time (s)
Basal Mean Circumferential Strain
Basal Mean Radial Strain
Equitorial Mean Circumferential Strain
Equitorial Mean Radial Strain
Apical Mean Circumferential Strain
Apical Mean Radial Strain

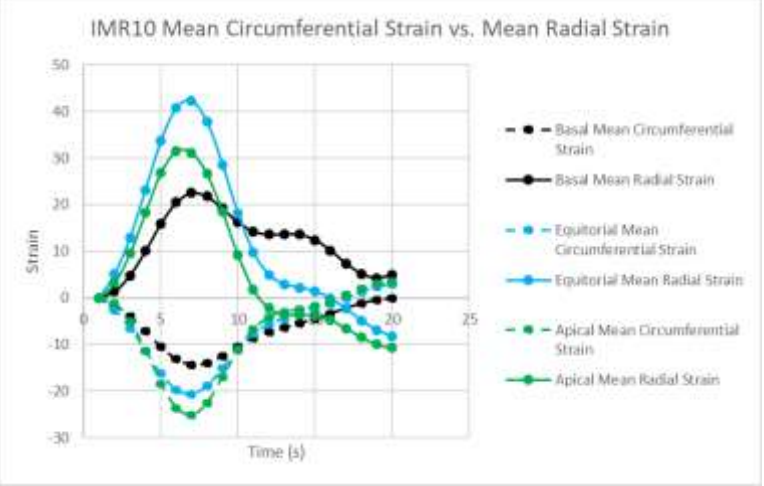
IMR10 Mean Circumferential Strain vs. Mean Radial Strain
Strain
Time (s)
Basal Mean Circumferential Strain
Basal Mean Radial Strain
Equitorial Mean Circumferential Strain
Equitorial Mean Radial Strain
Apical Mean Circumferential Strain
Apical Mean Radial Strain

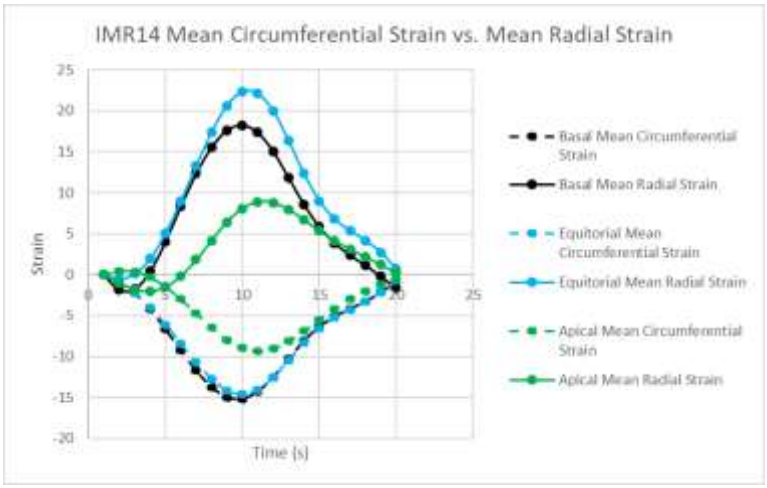

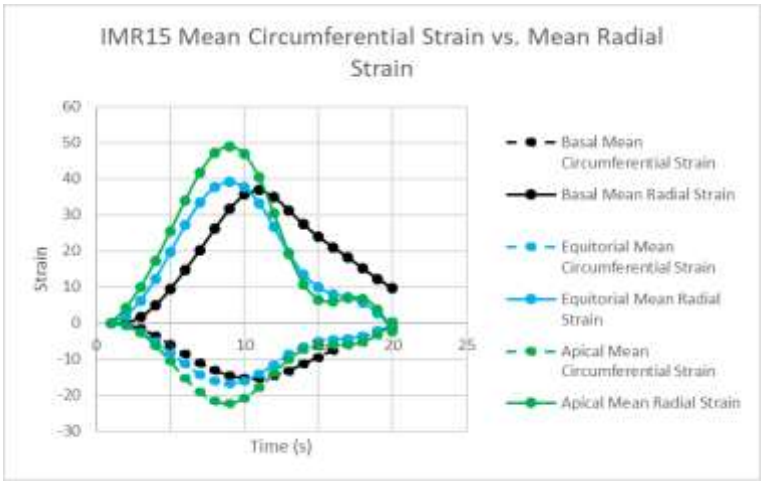

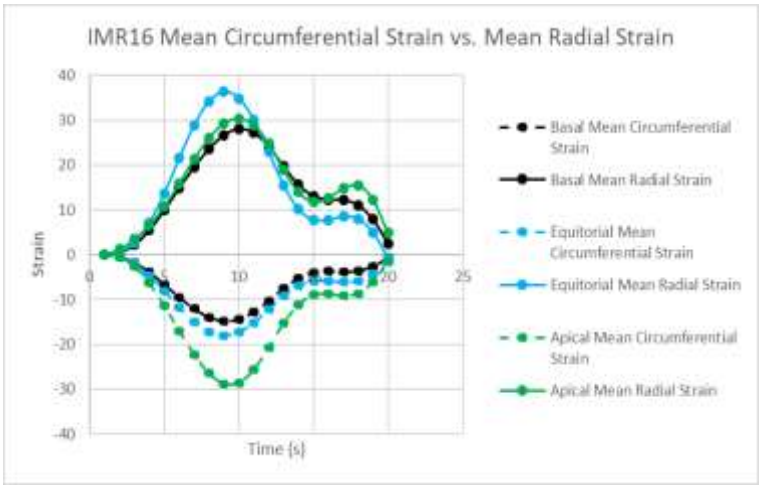

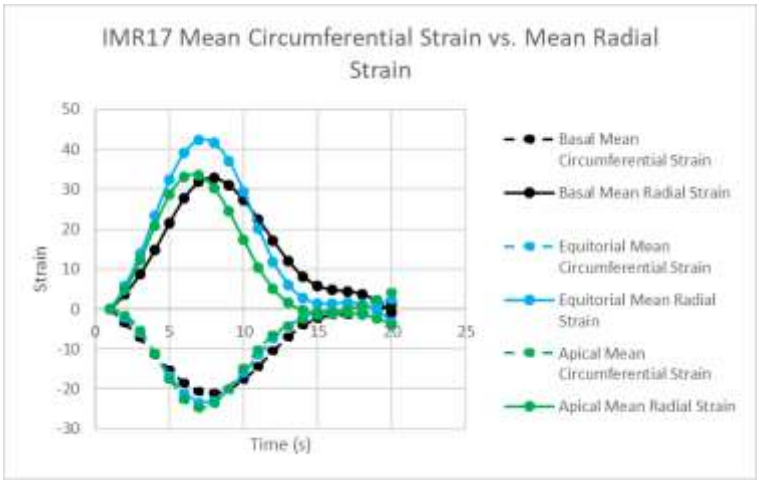

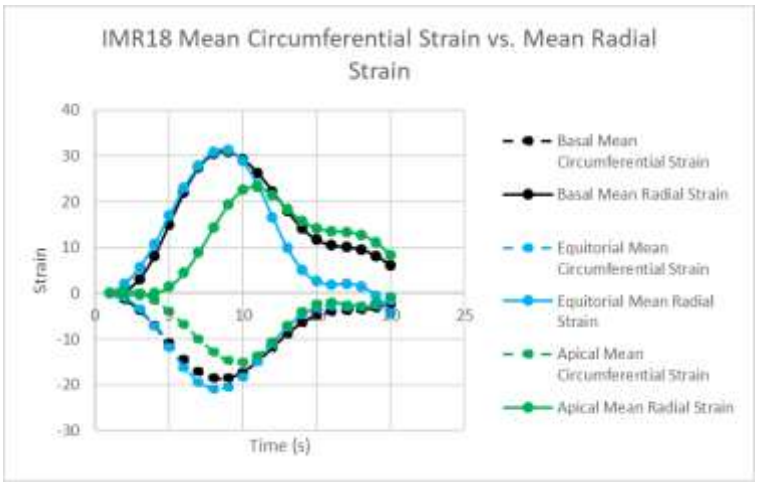

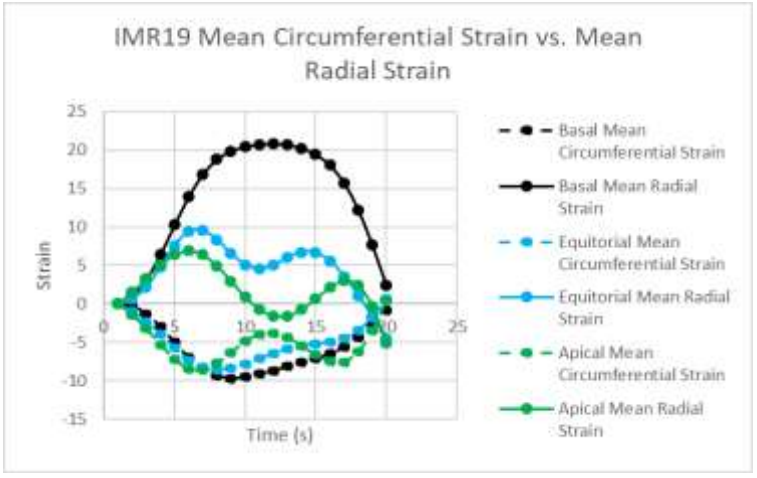

Figures 10-21: This group of figures (beginning with IMR 03 and ending with IMR19 in sequential order) shows the mean circumferential strain (dashed lines) and mean radial strain (solid lines) for all slices

segmented. Basal slices are shown in black, equatorial slices are shown in blue, and apical slices are shown in green. The general trends are evaluated in the discussion section.

Table 2: Peak mean circumferential strain and peak mean radial strain for basal, equatorial, and apical slices.

(Basal)	**IMR03**	**IMR05**	**IMR06**	**IMR07**	**IMR08**	**IMR10**
Peak Mean Circumferential Strain	-13.2666	-12.101	-18.6094	-14.1607	-24.4615	-14.341
Peak Mean Radial Strain	23.65743	24.80918	38.63005	34.05608	59.53872	22.53037
(Equatorial)						
Peak Mean Circumferential Strain	-11.6731	-14.0616	-19.8044	-10.7504	-32.7456	-20.6881
Peak Mean Radial Strain	26.54165	24.7093	39.17755	24.54898	70.52113	42.2511
(Apical)						
Peak Mean Circumferential Strain	-8.37886	-13.3742	-28.0552	-12.3033	-36.0955	-25.116
Peak Mean Radial Strain	21.00836	25.55984	32.03233	31.34163	59.70045	31.50744
(Basal)	**IMR14**	**IMR15**	**IMR16**	**IMR17**	**IMR18**	**IMR19**
Peak Mean Circumferential Strain	-15.1452	-15.4232	-14.7795	-21.0799	-18.567	-9.6659
Peak Mean Radial Strain	18.27353	36.83629	28.00408	32.79171	30.841114	20.82769
(Equatorial)						
Peak Mean Circumferential Strain	-14.619	-16.766	-18.0114	-23.2761	-20.89	-7.7881
Peak Mean Radial Strain	22.32571	39.14492	36.31635	42.24023	31.30918	9.52757
(Apical)						
Peak Mean Circumferential Strain	-9.34345	-22.2853	-28.8118	-24.8047	-15.1183	-8.5793
Peak Mean Radial Strain	8.888635	49.08389	30.34102	33.44462	23.21132	6.923067

CHAPTER 4

DISCUSSION

Strain Analysis of LV

This project used computational methods to evaluate regional LV contractile function in ischemic mitral regurgitation (IMR). Strain measurement, defined as the change in length in a specific direction over the original length, was used to understand LV contractility. On the short-axis view of the LV, the myocardium thickens during systole, giving positive values for radial strains. This is contrasted by the shortening of the circumference of the LV myocardium during systole, which results in negative values for circumferential strains. The entire LV is broken down into basal, equatorial, and apical levels. At each level the myocardium is further divided into anterior, anteroseptal, inferolateral, inferior, inferolateral, and anterolateral pieces. The radial and circumferential strains were analyzed at all these locations in this report.

It should be noted that this retrospective clinical trial is still being conducted and therefore patients must remain anonymous in order to prevent bias from entering the investigation.

Future Work

Future work on this project will include finishing the manual segmentation of MRIs for the remaining 54 patients and documenting primary and secondary outcome measures. Strain analysis will then be conducted with those patients as they were with the initial 12 in this paper. The final steps to investigating the hypotheses posed by this investigator will then include revealing the patients and their respective history of treatments and disease severity and analyzing both leaflet and ventricular geometry using echocardiography. Once a clear answer to these questions is obtained, surgeons will be consulted in order to bring these understandings to clinical applications.

REFERENCES

1. Kalam K, Otahal P, Marwick TH. Prognostic implications of global LV dysfunction: a systematic review and meta-analysis of global longitudinal strain and ejection fraction. *Heart (British Cardiac Society).* 2014;100(21):1673-1680.
2. Varma PK, Krishna, N., Jose, R. L., & Madkaiker, A. N. Ischemic mitral regurgitation. *Annals of cardiac anaesthesia.* 2017;20(4):432-439.
3. Chaput M, Handschumacher Mark D, Tournoux F, et al. Abstract 1745: Mitral Leaflet Adaptation to Ventricular Remodeling: Occurrence and Adequacy in 80 Patients With Functional Mitral Regurgitation. *Circulation.* 2007;116(suppl_16):II_368-II_368.
4. Borger MA. Ischemic Mitral Regurgitation: Why, When, and How? *CTSNet.* 2017.
5. Frantz E, Weininger F, Oswald H, Fleck E. Predictors for mitral regurgitation in coronary artery disease. In: *Ischemic mitral incompetence.* Springer; 1991:57-73.
6. Hickey MS, Smith LR, Muhlbaier LH, et al. Current prognosis of ischemic mitral regurgitation. Implications for future management. *Circulation.* 1988;78(3 Pt 2):I51-59.
7. Borger MA, Alam A, Murphy PM, Doenst T, David TE. Chronic Ischemic Mitral Regurgitation: Repair, Replace or Rethink? *The Annals of Thoracic Surgery.* 2006;81(3):1153-1161.
8. Kalra K WQ, McIver BV, et al. Temporal Changes in Interpapillary Muscle Dynamics as an

Active Indicator of Mitral Valve and Left Ventricular Interaction in Ischemic Mitral Regurgitation. *Journal of the American College of Cardiology.* 2014;64(18):1867-1879.

9. Frater RWM. The effects on cordal and leaflet stiffness of severe apical, posterior, and outward papillary displacement in advanced ventricular mechanism heart failure and mitral insufficiency. *J Heart Valve Dis.* 2011;20(6):608-618.
10. Ottavio Alfieri MDB. Repair options for mitral regurgitation *European Cardiology* 2011;7(2):131-135.
11. Bax Jeroen J, Braun J, Somer Soeresh T, et al. Restrictive Annuloplasty and Coronary Revascularization in Ischemic Mitral Regurgitation Results in Reverse Left Ventricular Remodeling. *Circulation.* 2004;110(11_suppl_1):II-103-II-108.
12. Braun J, van de Veire NR, Klautz RJ, et al. Restrictive mitral annuloplasty cures ischemic mitral regurgitation and heart failure. *Ann Thorac Surg.* 2008;85(2):430-436; discussion 436-437.
13. Bothe W, Miller DC, Doenst T. Sizing for mitral annuloplasty: where does science stop and voodoo begin? *The Annals of thoracic surgery.* 2013;95(4):1475-1483.
14. Kono T, Sabbah HN, Rosman H, Alam M, Jafri S, Goldstein S. Left ventricular shape is the primary determinant of functional mitral regurgitation in heart failure. *Journal of the American College of Cardiology.* 1992;20(7):1594-1598.

15. Bach DS, Bolling SF. Early improvement in congestive heart failure after correction of secondary mitral regurgitation in end-stage cardiomyopathy. *American Heart Journal.* 1995;129(6):1165-1170.
16. Izumi S, Miyatake K, Beppu S, et al. Mechanism of mitral regurgitation in patients with myocardial infarction: a study using real-time two-dimensional Doppler flow imaging and echocardiography. *Circulation.* 1987;76(4):777-785.
17. Magne J, Sénéchal M, Mathieu P, Dumesnil JG, Dagenais F, Pibarot P. Restrictive Annuloplasty for Ischemic Mitral Regurgitation May Induce Functional Mitral Stenosis. *Journal of the American College of Cardiology.* 2008;51(17):1692-1701.
18. Schwammenthal E, Vered Z, Agranat O, Kaplinsky E, Rabinowitz B, Feinberg Micha S. Impact of Atrioventricular Compliance on Pulmonary Artery Pressure in Mitral Stenosis. *Circulation.* 2000;102(19):2378-2384.
19. Zieliński T, Pogorzelska H, Rajecka A, Biedermavn A, Sliwiński M, Korewicki J. Pulmonary hemodynamics at rest and effort, 6 and 12 months after mitral valve replacement: a slow regression of effort pulmonary hypertension. *International Journal of Cardiology.* 1993;42(1):57-62.
20. Mihos CG, Yucel E, Santana O. The role of papillary muscle approximation in mitral valve repair for the treatment of secondary mitral regurgitation. *European Journal of Cardio-Thoracic Surgery.* 2016;51(6):1023-1030.
21. Mihos CG, Capoulade R, Yucel E, Melnitchouk S, Hung J. Combined papillary muscle sling and ring annuloplasty for moderate-to-severe secondary mitral regurgitation. *Journal of Cardiac Surgery.* 2016;31(11):664-671.
22. Roshanali F, Vedadian A, Shoar S, Naderan M, Mandegar MH. Effi cacy of papillary muscle approximation in preventing functional mitral regurgitation recurrence in high-risk patients with ischaemic cardiomyopathy and mitral regurgitation. *Acta Cardiologica.* 2013;68(3):271-278.
23. Mihos CG, Pineda AM, Santana O. Targeting the papillary muscles in mitral valve repair for ischemic mitral regurgitation. *Rev Cardiovasc Med.* 2015;16(3):182-188.
24. Mihos CG, Yucel E, Santana O. The role of papillary muscle approximation in mitral valve repair for the treatment of secondary mitral regurgitation. *European journal of cardio-thoracic surgery : official journal of the European Association for Cardio-thoracic Surgery.* 2017;51(6):1023-1030.
25. Kim K, Kaji S, An Y, et al. Interpapillary muscle distance independently affects severity of functional mitral regurgitation in patients with systolic left ventricular dysfunction. *The Journal of Thoracic and Cardiovascular Surgery.* 2014;148(2):434-440.e431.
26. Nappi F, Spadaccio C, Chello M, Mihos CG. Papillary muscle approximation in mitral valve repair for secondary MR. *J Thorac Dis.* 2017;9(Suppl 7):S635-S639.
27. Mandinov L, Büllesfeld L, Kuck K-H, Grube E. *Early Insight into Mitralign Direct Annuloplasty for Treatment of Functional Mitral Regurgitation.* Vol 62011.
28. McGee EC, Jr., Gillinov AM, Blackstone EH, et al. Recurrent mitral regurgitation after annuloplasty for functional ischemic mitral regurgitation. *The Journal of Thoracic and Cardiovascular Surgery.* 2004;128(6):916-924.

29. Magne J, Pibarot P, Dagenais F, Hachicha Z, Dumesnil Jean G, Sénéchal M. Preoperative Posterior Leaflet Angle Accurately Predicts Outcome After Restrictive Mitral Valve Annuloplasty for Ischemic Mitral Regurgitation. *Circulation.* 2007;115(6):782-791.
30. Julien Magne PP, François Dagenais , Zeineb Hachicha , Jean G. Dumesnil , and Mario Sénéchal. Preoperative Posterior Leaflet Angle Accurately Predicts Outcome After Restrictive Mitral Valve Annuloplasty for Ischemic Mitral Regurgitation. *Circulation.* 2007;115:782-791.
31. Levine RA. Dynamic Mitral Regurgitation — More Than Meets the Eye. *New England Journal of Medicine.* 2004;351(16):1681-1684.
32. Omran AS, Arifi AA, Mohamed AA. Echocardiography of the mitral valve. *Journal of the Saudi Heart Association.* 2010;22(3):165-170.
33. Seth Uretsky M. Quantification of Mitral Regurgitation Using MRI. *American College of Cardiology* 2016.
34. Mehta NK, Kim J, Siden JY, et al. Utility of cardiac magnetic resonance for evaluation of mitral regurgitation prior to mitral valve surgery. *J Thorac Dis.* 2017;9(Suppl 4):S246-S256.
35. Ehlers AP, Khor S, Shonnard N, et al. Intra-Wound Antibiotics and Infection in Spine Fusion Surgery: A Report from Washington State's SCOAP-CERTAIN Collaborative. *Surgical infections.* 2016;17(2):179-186.
36. Smiseth OA, Torp H, Opdahl A, Haugaa KH, Urheim S. Myocardial strain imaging: how useful is it in clinical decision making? *Eur Heart J.* 2016;37(15):1196-1207.
37. Morais P, Marchi A, Bogaert JA, et al. Cardiovascular magnetic resonance myocardial feature tracking using a non-rigid, elastic image registration algorithm: assessment of variability in a real-life clinical setting. *J Cardiovasc Magn Reson.* 2017;19(1):24-24.